ISSN 1330-3651 (Print), ISSN 1848-6339 (Online)
https://doi.org/10.17559/TV-20181213180042
Original scientific paper

Effect of Nb Additive on the Dynamic Compression Property of a Zr-Ta Alloy

Wei HAN, Yong HE, Chuanting WANG, Zhiping GUO, Xiaojun SHEN, Yuan HE

Abstract: In this paper, Ta50-Zr50 and Ta45-Zr45-Nb10 alloys were compounded by casting. Quasi-static and dynamic compression tests were applied for both alloys, and also the role of Nb additive on the mechanical property of Zr-Ta alloy, was studied. The microstructure characterization demonstrated that both alloys had relative homogeneous structure with micro-laminate structure inside grains. The Nb additives increased the strength of the alloy by various strain rates, while the ductility of the alloys was decreased. The various parameters of constitutive equations for both alloys were obtained by fitting data. The constitutive equations are applied in theoretical models, the simulation software helps to predict the strength of alloy through various strain rates.

Keywords: constitutive model; dynamic compression; Zr-Ta alloy

1 INTRODUCTION

Refractory metal alloy coatings, such as Ta-Ru and Ta-Zr coatings, are widely applied as surface protection for high-temperature molding dies. Ta-Zr coatings are widely used to enhance the service lifetime of the die materials because of their high hardness, phase stability and oxidation resistance [1-5]. Extensive studies have been reported on producing Ta-Zr alloy films via coating technology, for instance, co-sputtering [1], co-condensation [4] and ion beam mixing and [5] etc.

Extensive studies were conducted on mechanical property and oxidation behavior of Ta-Zr alloy films. An amorphous structure was obtained on a Ta-Zr alloy film, which was produced by co-sputting [1]. Results have shown that the hardness of Ta-Zr alloy film could be significantly improved to 13 GPa, after oxidation treatment at 873 K due to formation of ZrO_2 phase [2]. A high hardness of 17 GPa was achieved on a Ta49-Zr51 alloy coating after annealing in a O_2-N_2 atmosphere, which makes such alloy a favorable candidate coating for molding dies [3].

Nevertheless, all previous studies have been focused on producing Ta-Zr alloy films with various coating technology, these Ta-Zr coatings have final thickness of less than 1 μm. The performance of Ta-Zr films could be limited due to their small thickness, especially in the work environment of molding dies. The difference of thermal property between Ta-Zr coating and substrate could lead to delamination or cracking of the coating after heating/cooling working cycle.

To date, there is no report on producing bulk Ta-Zr alloy via casting. This paper has aimed to investigate the mechanical property of a cast Ta-Zr alloy, especially the effect of Nb on the mechanical property of the Ta-Zr alloys.

2 EXPERIMENTS

The Ta-Zr and Ta-Zr-Nb alloy were produced by melting the pure elements together under a purified Ar atmosphere.

Samples for microstructure observation were polished by abrasive papers to 1600 grit, then to 1 μm using a diamond suspension, detached by using a solution of $HF:HNO_3:H_2O$=1:4:45. The microstructure was analyzed by scanning electron microscopy (JEOL JSM 6500) under high voltage of 15 kV.

Cylindrical samples (∅3×6 mm) have been machined from the alloy ingot for quasi-static compression test. Testing machine of Universal materials has been employed for the compression test. The tests have been performed under a nominal initial strain rate of 10^{-4} to 10^{-2} s^{-1}.

Split Hopkinson Pressure Bar (SHPB) test was conducted to study dynamic compression behavior of samples under high strain rates, the principles of SHPB test have been reported earlier [6-10]. The experimental device is mainly composed of the loading device, some of the bars and the data acquisition system [11, 12]. Cylindrical specimen (∅6×3 mm) has been machined for dynamic compression tests. The dynamic compression tests have been conducted at the average strain rates from 500 to 3000 s^{-1}.

3 RESULTS

Fig. 1 shows the microstructure of Ta-Zr and Ta-Zr-Nb alloys. As shown in Fig. 1, the mean grain size of alloy is between 40 and 50 μm. Due to the low solubility of Ta and Zr, the two elements formed micro-laminate structure inside grains, the space among laminar was around several tens of nanometers, which indicated that the Ta and Zr elements have been homogeneously distributed inside each grain of the alloy. The microstructure of the Ta-Zr and Ta-Zr-Nb alloys is different from those films produced via coating technology. Such laminate structure inside large grains was formed during solidification, while the coating technology tends to form packed pure metal layers or amorphous structures [1-5].

Fig. 2 shows the compression engineering stress-strain and corresponding true stress-strain curves of the Ta-Zr and Ta-Zr-Nb alloy. The yield stress, ultimate compression stress, and elongation to failure of Ta50-Zr50 alloy is around 900 MPa, 1800 MPa and 35%, respectively. The yield stress, ultimate compression stress, and elongation to failure of Ta45-Zr45-Nb10 alloy is around 1000 MPa, 1600 MPa and 17%, respectively. It is obvious that as the Nb elements were added into the alloy, the yield strength of the alloy has improved while the ductility of the alloy has reduced remarkably.

The strain in the SHPB testing was measured by a strain gauge. The strain gage signal has been adjusted by a Wheatstone bridge and amplified by an amplifier to obtain the final voltage signal. Based on the recorded incident reflection and transmission curve, the true strain, stress rate are calculated. Fig. 3(a) shows the voltage signal on the strain gauge collected by the oscilloscope during the SHPB test, the result shows that the intensity of transmitted and reflected waves increases with the accelerating of the impact velocity. According to Fig. 3(a), the wave pattern exhibits good regularity and achieves constant strain rate loading. Compared with the quasi-static test results, the dynamic yield stress is higher than the yield stress of the quasi-static test, as shown in Fig. 3(b). The enhancement effect of strain rate is not obvious with the increase of strain rate. As the strain rate increases, the plastic stage of the material becomes longer, fracture occurs when plastic deformation reaches a certain value [6-8].

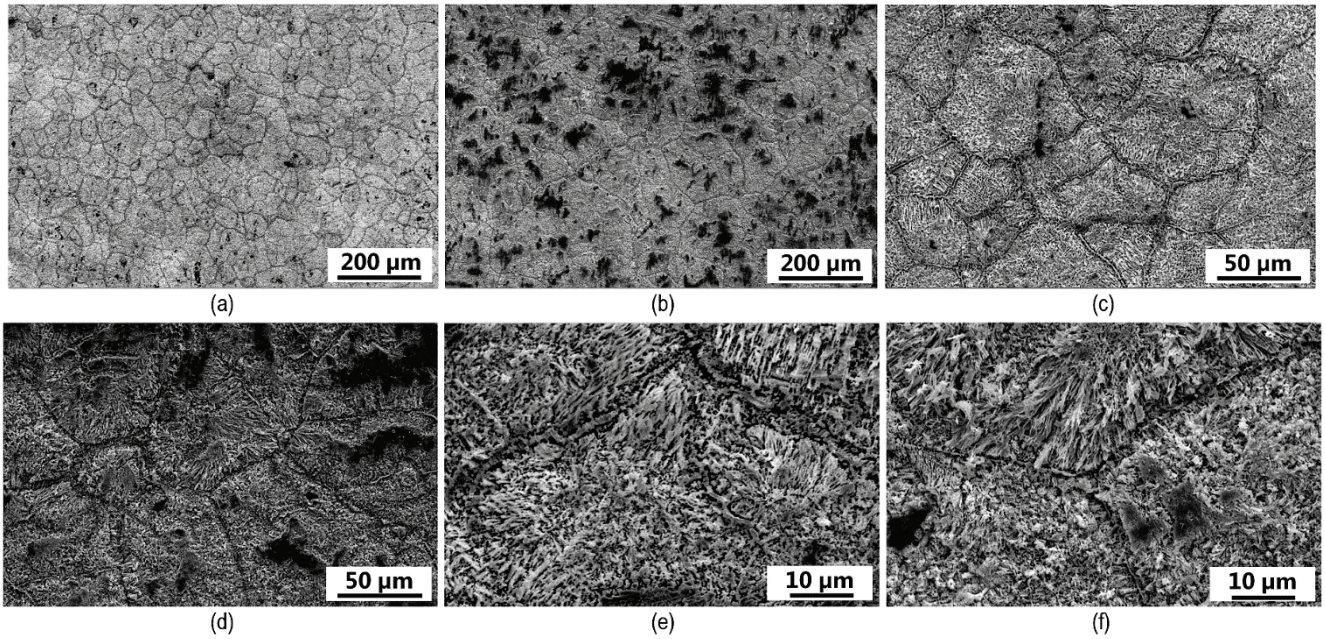

Figure 1 Microstructure of Ta50-Zr50 (a, c, e), Ta45-Zr45-Nb10 (b, d, f) under various magnification

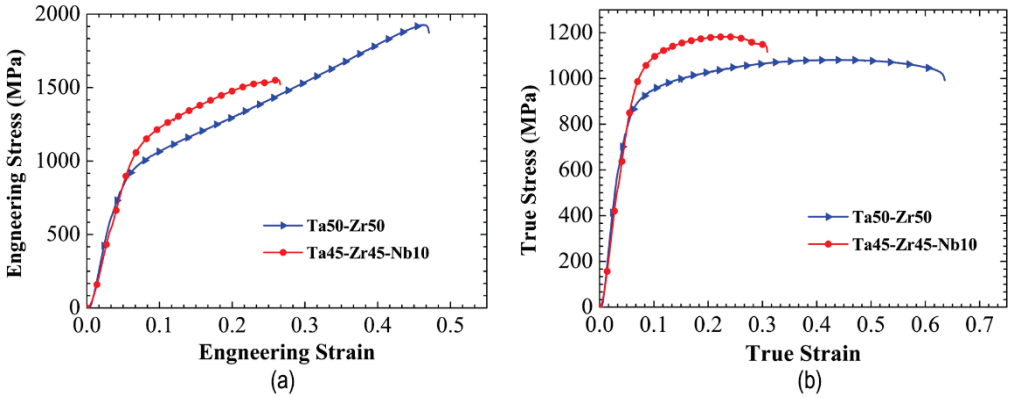

Figure 2 The compression engineering stress-strain (a) and corresponding true stress-strain curves (b) of the Ta-Zr and Ta-Zr-Nb alloy under quasi-static deformation at room temperature

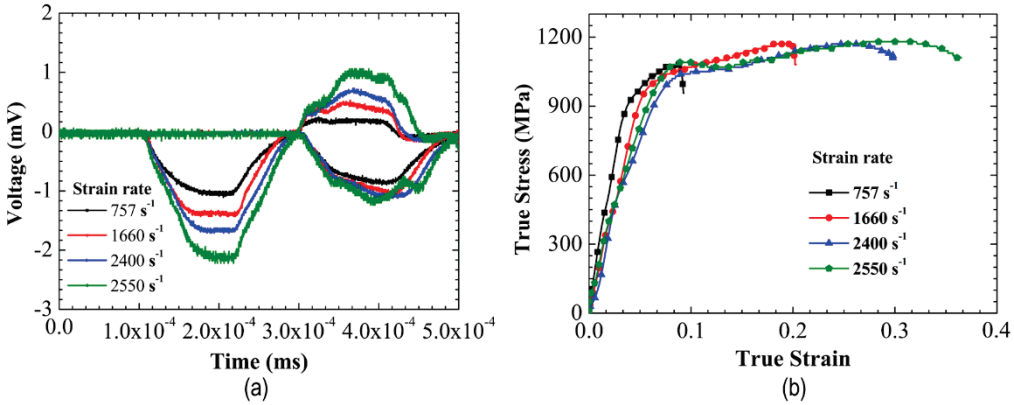

Figure 3 The voltage signal (a) and corresponding true stress-strain curves (b) of Ta50-Zr50 alloy under dynamic compression

Fig. 4 (a) shows the voltage signal on the strain gauge collected by the oscilloscope during the SHPB test of Ta45-Zr45-Nb10, and the figure 4(b) is the stress-strain curve of Ta45-Zr45-Nb10 alloy at different strain rates. Compared with Ta50-Zr50, the yield strength of Ta45-Zr45-Nb10 is higher, while plasticity is not as good as that of Ta50-Zr50. The dynamic yield strength of Ta45-Zr45-Nb10 is significantly higher than that of static yield strength. As the strain rate increases, fracture of Ta45-Zr45-Nb10 will occur. The Ta50-Zr50 alloy is under plastic deformation under a similar strain rate.

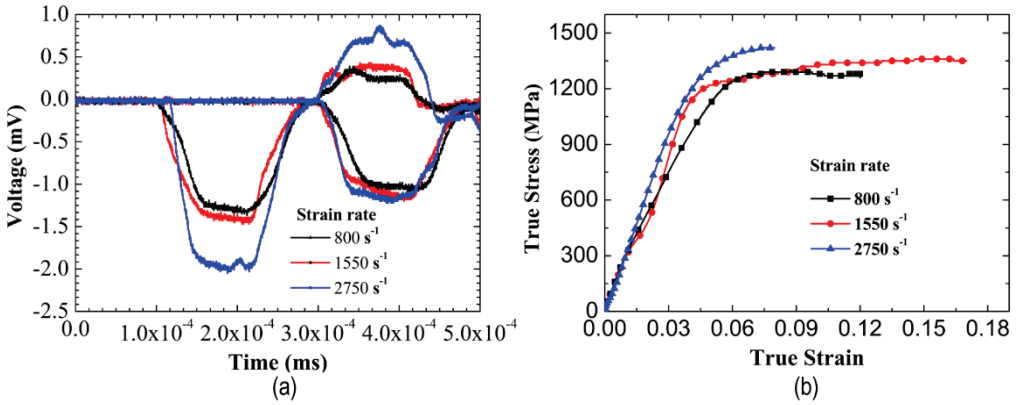

Figure 4 The voltage signal (a) and corresponding true stress-strain curves (b) of Ta45-Zr45-Nb10 alloy under dynamic compression.

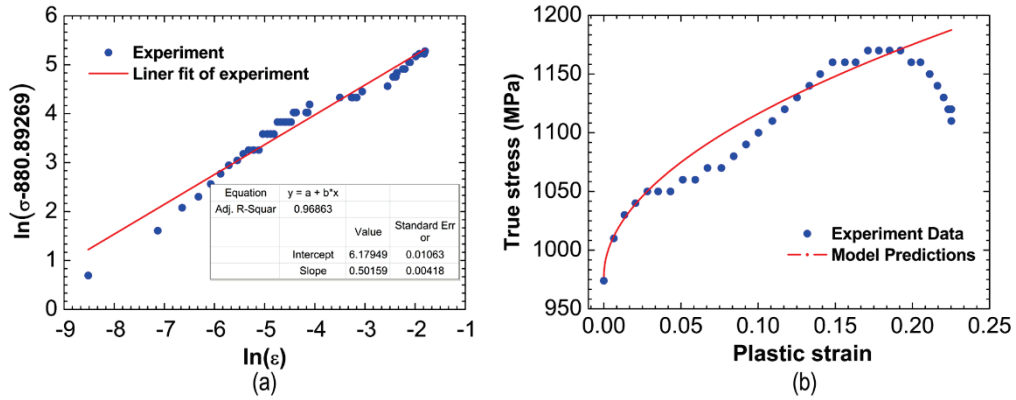

Figure 5 The fitting results of parameters n and B (a) and the true stress versus plastic strain of Ta50-Zr50 under strain rate of 1660 s^{-1} (b).

4 DISCUSSION

The constitutive models proposed by Zerilli and Armstrong (Z-A), Johnson and Cook (J-C), Steinberg et al. (S-G) refer to the mathematical model of the macroscopic mechanical properties of materials [13-15]. The J-C model shows acceptable accuracy to describe the dynamic mechanical behavior of pure tantalum and tantalum alloys [16, 17]. The J-C strength model is an empirical model, which contains the effects of strain, strain rate, and temperature on the dynamic mechanical behavior of materials:

$$\sigma = \left[A + B \cdot (\varepsilon^p)^n\right] \cdot \left[1 + C \cdot \ln(\dot{\varepsilon}^*)\right] \cdot \left[1 - T^{*m}\right] \quad (1)$$

where $T^* = \dfrac{T - T_r}{T_m - T_r}$, T, T_r, T_m is the ambient temperature, the room temperature, the melting point, respectively. ε^p is the effective plastic strain, $\dot{\varepsilon}^* = \dot{\varepsilon}/\dot{\varepsilon}_0$ the dimensionless strain rate, A, B, C, n, m are all undetermined coefficients, which can be fitted by experimental values. The constant A is the basic yield stress under low strain, while B and N indicate strain-hardening effect. Under the reference strain rate and the reference temperature, the initial yield stress A, the hardening modulus B and the hardening exponent n can be obtained by the quasi-static experiment. In order to determine the temperature softening coefficient m, the stress curves under the same strain rate under the Hopkinson bar experiment and the quasi-static strain rate can be used, and a number of experimental data of dynamic mechanics can obtain the parameter C.

In this paper, under the condition of room temperature and strain rate of 757 s^{-1}, the true stress-strain curve obtained in the quasi-static compression experiment is used, and the J-C strength constitutive model can be simplified as follows:

$$\sigma = (A + B \cdot \varepsilon^n) \cdot \left[1 + C \cdot \ln\left(\frac{\dot{\varepsilon}}{\dot{\varepsilon}_0}\right)\right] \quad (2)$$

For Ta50-Zr50 alloy, when the strain is 0.5%, the stress corresponding to the curve is approximately the yield strength of the material, and the $A = 0.5\sigma = 880.89269$ MPa can be determined from Fig. 2.

The σ-ε curve is converted into a $\ln(\sigma - 880.89269) - \ln(\varepsilon)$ curve by Origin software, the intercept of the curve is

ln(B) and the slope is n, thus the value of B and N is determined.

The fitting of parameter n and B is shown in Fig. 5(a), the fitting curve is close to the experimental data. Tab. 1 shows that the fitting parameters, fitting correlation coefficients, and the fitting correlation coefficients are close to 1.

Therefore, it can be obtained that $B = e^{6.17949} = 482.74569$ MPa, $n = 0.50159$.

The stress-strain relationship of Ta50-Zr50 at room temperature can be obtained by substituting A, B and n into Eq. (2):

$$\sigma = \left(880.89269 + 482.74569 \cdot \varepsilon^{0.50159}\right) \cdot \left[1 + C \cdot \ln\left(\frac{\dot{\varepsilon}}{\dot{\varepsilon}_0}\right)\right] \quad (3)$$

Fig. 5(a) shows the true stress versus plastic strain after yield point for Ta50-Zr50 alloy under strain rate of 1660 s^{-1}.

When the strain is zero, Eq. (3) can be transformed into

$$\frac{\sigma}{880.89269} - 1 = C \cdot \ln\left(\frac{\dot{\varepsilon}}{\dot{\varepsilon}_0}\right) \quad (4)$$

By plotting the curve of $\frac{\sigma}{880.89269} - 1$ versus $C \cdot \ln\left(\frac{\dot{\varepsilon}}{\dot{\varepsilon}_0}\right)$, the parameter C can be determined, as shown in Fig. 6 and Tab. 2.

The constitutive equation of Ta50-Zr50 can be written as:

$$\sigma = \left(880.89269 + 482.74569 \cdot \varepsilon^{0.50159}\right) \cdot \left[1 + 0.1067 \cdot \ln\left(\frac{\dot{\varepsilon}}{\dot{\varepsilon}_0}\right)\right] \quad (5)$$

Similarly, the constitutive equation of Ta45-Zr45-Nb10 can be written as：

$$\sigma = \left(1100.0138 + 591.98423 \cdot \varepsilon^{0.51083}\right) \cdot \left[1 + 0.1066 \cdot \ln\left(\frac{\dot{\varepsilon}}{\dot{\varepsilon}_0}\right)\right] \quad (6)$$

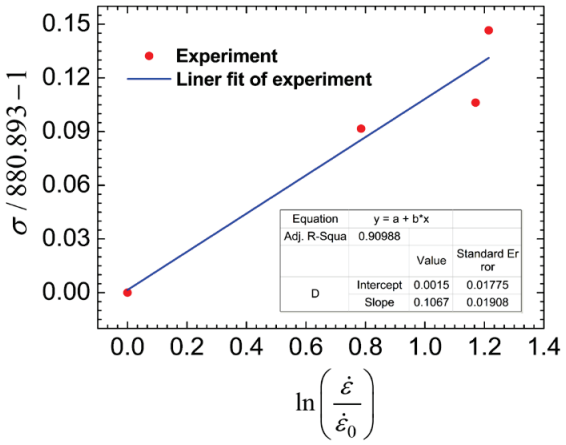

Figure 6 The experimental and fitting results of parameters C of Ta50-Zr50

The constitutive equations of both alloys are shown in Eq. (5) and Eq. (6), which can be applied in theoretical models and simulation software to predict the strength of alloy under various stain rates.

Table 1 The values of parameters A and B forTa50-Zr50 alloy

	Value	Std err	R^2
n	0.50159	0.00418	0.96863
ln(B)	6.17949	0.01063	0.96863

Table 2 The fitting results of parameters C of Ta50-Zr50

	Value	Std error	R^2
C	0.1067	0.01908	0.90988

5 CONCLUSION

Ta-Zr and Ta-Zr-Nb bulk alloy is obtained via casting for the first time. Quasi-static and dynamic compression tests were applied on a Ta50-Zr50 and Ta45-Zr45-Nb10 alloy. The conclusions are as follows:

1. Both alloys showed relative homogeneous structure with micro-laminate structure inside grains.

2. The Nb additives increased the yield strength of the alloy under various strain rates, while the ductility of the alloys was decreased.

3. The constitutive equations obtained for both alloys can be applicable in theoretical models and simulation software to predict the strength of alloy under various stain rate.

Acknowledgements

The National Natural Science Foundation of Jiangshu China (BK20160832) and the National Natural Science Foundation of China (No. 51601095, No. 11504173, No. 11502118, No. 11702145, No. 51375244, and No. 51301093) funded this work.

6 REFERENCES

[1] Chen, Y. I. & Chen, S. M. (2013). Annealing effects on nanostructure and mechanical properties of nanolaminated Ta-Zr coatings. *Surface & Coatings Technology*, 215, 209-217. https://doi.org/10.1016/j.surfcoat.2012.08.074

[2] Chen, Y. I. & Chen, S. M. (2013). Oxidation study of Ta-Zr coatings. *Thin Solid Films*, 529, 287-291. https://doi.org/10.1016/j.tsf.2012.03.088

[3] Tang, Z. Z., Hsieh, J. H., Zhang, S. Y., Li, C., & Fu, Y. Q. (2005). Phase transition and microstructure change in Ta-Zr alloy films by co-sputtering. *Surface & Coatings Technology*, 198, 110-113. https://doi.org/10.1016/j.surfcoat.2004.10.019

[4] Hecht, H., Weigang, G., Eichert, S., & Geyer, U. (1996). Formation area of thin amorphous Zr-Mn and Zr-Ta films prepared by cocondensation. *Zeitschrift für Physik B Condensed Matter*, 100, 47-51. https://doi.org/10.1007/s002570050092

[5] Jin, O. & Liu, B. X. (1997). Chemical and interface effects on glass forming ability under ion mixing in Zr-Ta system of positive heat of formation. *Journal of Non-Crystalline Solids*, 211, 180-186. https://doi.org/10.1016/S0022-3093(96)00576-5

[6] Zou, D. L., Luan, B. F., Liu, Q., Chai, L. J., & Chen, J. W. (2012). Characterization of adiabatic shear bands in the zirconium alloy impacted by split Hopkinson pressure bar at a strain rate of 6000 s^{-1}. *Materials Science & Engineering A*, 558, 517–524. https://doi.org/10.1016/j.msea.2012.08.038

[7] Sudheera, Rammohan, Y. S., & Pradeep, M. S., (2018). Split

Hopkinson Pressure Bar Apparatus for Compression Testing: A Review. *Materials Today: Proceedings*, 5, 2824-2829.
[8] Nurel, B., Nahmany, M., Frage, N., Stern, A., & Sadot, O. (2018). Split Hopkinson pressure bar tests for investigating dynamic properties of additively manufactured AlSi10Mg alloy by selective laser melting. *Additive Manufacturing*, 22, 823-833. https://doi.org/10.1016/j.addma.2018.06.001
[9] Zhao, H. & Gary, G. (1996). On the use of the SHPB techniques to determine the dynamic behavior of materials in the range of small strains. *International Journal of Solids and Structures*, 28, 1-7. https://doi.org/10.1016/0020-7683(95)00186-7
[10] Meyers, M. A. (1994). *Dynamic Behavior of Materials*, John Wiley & Sons, New York. https://doi.org/10.1002/9780470172278
[11] Lee, O. S. & Kim, M. S. (2003). Dynamic material property characterization by using split Hopkinson pressure bar (SHPB) technique. *Nuclear Engineering and Design*, 226, 119-125. https://doi.org/10.1016/S0029-5493(03)00189-4
[12] Chen, W. B. (2011). *Split Hopkinson (Kolsky) bar, design, tesing and application*, Springer, New York. https://doi.org/10.1007/978-1-4419-7982-7
[13] Zerilli, P. J. & Armstrong, R. W. (1987). Dislocation-mechanics-based constitutive relations WH. A for material dynamics calculations. *Journal of Applied Physics*, 61, 1816-1825. https://doi.org/10.1063/1.338024
[14] Johnson, G. R. (1983). Cook constitutive model and data for metals subjected to large strains, high strain rates and high temperatures. *Proceedings of the 7th International Symposium on Ballistics, 21*(1), 541-547.
[15] Steinberg, D. J., Cochran, S. G., Guinan, M. W. (1980). A constitutive model for metals applicable at high-strain rate. *Journal of Applied Physics, 51*(3), 1498-1504. https://doi.org/10.1063/1.327799
[16] Bai, R., Zhang, X. M. et al. (2008). Dynamic Behavior and Constitutive Model of Tantalum Tungsten Alloy. *Rare Metal Materials and Engineering, 37*(9), 1526-1529.
[17] Peng, J. X., Li, Y. L., & Li, D. H. (2003). An experimental study on the dynamic constitutive relation of tantalum. *Explosion & Shock Waves, 23*(2), 183-187.

Contact information:

Wei HAN
School of Mechanical Engineering,
Nanjing University of Science & Technology,
Nanjing, Jiangsu, 210094, P. R. China
Beijing Special Electromechanical Research Institute,
Beijing, 100081, P. R. China

Yong HE
School of Mechanical Engineering,
Nanjing University of Science & Technology,
Nanjing, Jiangsu, 210094, P. R. China

Chuanting WANG
(Corresponding author)
School of Mechanical Engineering,
Nanjing University of Science & Technology,
Nanjing, Jiangsu, 210094, P. R. China
E-mail: ctwang@njust.edu.cn

Zhiping GUO
School of Mechanical Engineering,
Nanjing University of Science & Technology,
Nanjing, Jiangsu, 210094, P. R. China

Xiaojun SHEN
School of Mechanical Engineering,
Nanjing University of Science & Technology,
Nanjing, Jiangsu, 210094, P. R. China
Beijing Special Electromechanical Research Institute,
Beijing, 100081, P. R. China

Yuan HE
School of Mechanical Engineering,
Nanjing University of Science & Technology,
Nanjing, Jiangsu, 210094, P. R. China